INL/JOU-15-35776
Accepted Manuscript

QUANTITATIVE EVALUATION OF AN AIR MONITORING NETWORK USING ATMOSPHERIC TRANSPORT MODELING AND FREQUENCY OF DETECTION METHODS

Arthur S. Rood, A. Jeffery Sondrup, Paul D. Ritter

April 2016

Prepared for the U.S. Department of Energy
Office of Nuclear Energy
Under DOE Idaho Operations Office
Contract DE-AC07-05ID14517

QUANTITATIVE EVALUATION OF AN AIR MONITORING NETWORK USING ATMOSPHERIC TRANSPORT MODELING AND FREQUENCY OF DETECTION METHODS

Arthur S. Rood*, A. Jeffery Sondrup†, Paul D. Ritter‡

Conflict of Interest: Authors declare no conflict of interest.
Source of Funding: U.S. Department of Energy, Idaho Field Office funded this project.

* Corresponding author, K-Spar Inc., 4835 W. Foxtrail Lane, Idaho Falls, Idaho 83402, Phone: 208 528-0670, asr@kspar.com
† Idaho National Laboratory, Idaho Falls, Idaho
‡ Bechtel BWTX Idaho, LLC.

ABSTRACT

A methodology has been developed to quantify the performance of an air-monitoring network in terms of frequency of detection. Frequency of detection is defined as the fraction of "events" that result in a detection at either a single sampler or network of samplers. An "event" is defined as a release to the atmosphere of a specified amount of activity over a finite duration that begins on a given day and hour of the year. The methodology utilizes an atmospheric transport model to predict air concentrations of radionuclides at the samplers for a given release time and duration. Another metric of interest determined by the methodology is called the network intensity, which is defined as the fraction of samplers in the network that have a positive detection for a given event. The frequency of detection methodology allows for evaluation of short-term releases that include effects of short-term variability in meteorological conditions. The methodology was tested using the U.S. Department of Energy Idaho National Laboratory Site ambient air monitoring network consisting of 37 low-volume air samplers in 31 different locations covering a 17,630 km^2 region. Releases from six major facilities distributed over an area of 1,435 km^2 were modeled and included three stack sources and eight ground-level sources. A Lagrangian Puff air dispersion model (CALPUFF) was used to model atmospheric transport. The model was validated using historical ^{125}Sb releases and measurements. Relevant one-week release quantities from each emission source were calculated based on a dose of 1.9×10^{-4} mSv at a public receptor (0.01 mSv assuming release persists over a year). Important radionuclides were ^{241}Am, ^{137}Cs, ^{238}Pu, ^{239}Pu, ^{90}Sr, and tritium. Results show the detection frequency was over 97.5% for the entire network considering all sources and radionuclides. Network intensity results ranged from 3.75% to 62.7%. Evaluation of individual samplers indicated some samplers were poorly located and added little to the overall effectiveness of the network. Using the frequency of detection methods, alternative sampler placements were simulated that could substantially improve the performance and efficiency of the network.

Keywords: atmospheric transport, atmospheric emissions, air monitoring, meteorological modeling, radiation monitoring.

INTRODUCTION

Ambient air monitoring networks are an important part of a facility's environmental monitoring program. They monitor for routine and unforeseen releases, provide verification that the facility is in compliance with radiological dose limits, and can be used to assess impact to the environment over time. The overall effectiveness of an air monitoring network is dependent on number and placement of samplers, flow rates and sampling times of the samplers, and analytical methods used to measure radionuclides in air. Placement of samplers based on the annual wind roses or annual average dispersion patterns provides a good first-cut at identifying favorable sampling locations. However, it does not provide a quantitative measure of the sampler or overall network performance for typical filter collection times (1-week), or for releases of short duration.

Earlier investigators (Pelletier 1968, Waite 1973) used methods linked to Gaussian Plume models to evaluate the probability of detecting a radionuclide release. Ritter et al. (2013) expanded upon this methodology and generalized it for use with a Lagrangian Puff dispersion model. The goal of the Ritter et al. (2013) study was to develop an objective measure of the performance (or effectiveness) of a regional network of air sampling stations as it is affected by: 1) the positions of samplers within the region relative to the positions of sources; 2) meteorology; and 3) air sampling/analysis parameters (i.e., flow rate, measurement sensitivity, and period for collection or compositing of sample collection media). Ritter et al. (2013) proposed the criterion for 'effectiveness' of a sampling network to be the likelihood that the activity collected by a minimum number of samplers in the network will exceed the minimum detectable activity (MDA). They also proposed the "likelihood of detection" could be based on an evaluation of the "frequency of detection." The frequency of detection is determined using a numerical air-dispersion model that utilizes multiple independent historical meteorological data sequences and simulates releases of constant activity, beginning at various times (1-hour resolution) and extending at a constant rate over various durations (1-hour increments), with each combination of release start time and duration corresponding to an equal potential time-integrated concentration (*TIC*) and offsite dose (actual *TICs* are dependent on actual meteorological conditions).

In this paper, the frequency of detection methodology described in Ritter et al. (2013) is generalized and fully implemented so that it can be applied using any appropriate atmospheric dispersion model. Meteorological data was on a 1-hour time resolution, but the methodology could be applied to finer time increments allowing for evaluation of sub-hour releases. The methodology is then applied to the existing sampling network at the Idaho National Laboratory (INL) using a Lagrangian Puff atmospheric dispersion model. Predicted concentrations from atmospheric transport model are compared with measurements to provide confidence in model results. Finally, the model and methodology are used to suggest measures that could be taken to optimize or improve the existing network.

Idaho National Laboratory Site

The U.S. Department of Energy (DOE) INL Site is a 2,305 km^2 reservation located on the Eastern Snake River Plain of southeastern Idaho, approximately 25 miles west of Idaho Falls (Fig. 1). Federal lands surround much of the INL Site, including Bureau of Land Management lands and Craters of the Moon National Monument to the southwest, Challis National Forest to the west, and Targhee National Forest to the north. About 60% of the INL Site is open to livestock grazing and hunting is permitted in a limited area on the northwest and northeast portions of the Site.

The INL was established in 1949 as the National Reactor Testing Station. The original mission of INL was to build, test, and operate various nuclear reactors and associated support facilities. Since 1949, the INL has designed and built 52 mostly first-of-their-kind nuclear reactors creating the largest concentration of reactors in the world. The isolated location ensured maximum public safety in the field of nuclear research. Today, INL is a multi-program laboratory that supports DOE missions and business lines of nuclear energy research, energy resources, science and technology, and national security. The INL Site consists of several primary facilities situated on an expanse of otherwise undeveloped terrain (Fig. 2). Buildings and structures at the INL Site are clustered within these facilities, which are typically less than 5 km^2 in size and separated from each other by kilometers of undeveloped land. The major facilities at the INL Site are the Advanced Test Reactor (ATR) Complex (ATRC); Central Facilities Area (CFA); Critical Infrastructure Test Range Complex (CITRC); Idaho Nuclear Technology and Engineering Center (INTEC); Materials and Fuels Complex (MFC); Naval Reactors Facility (NRF); Radioactive Waste Management Complex (RWMC); and Test Area North (TAN), which includes the Specific Manufacturing Capability (SMC).

Air Monitoring Network

The INL Site ambient air-monitoring network consists of 37 low-volume air samplers in 31 different locations (Fig. 1). Twenty-one samplers with the BEA prefix are operated by Battelle Energy Alliance (BEA), and 16 samplers with the ESER prefix are operated by the Environmental Surveillance, Education, and Research (ESER) program. There are collocated samplers at Craters of the Moon National Monument, Sugar City, Blackfoot, Idaho Falls, Van Buren Avenue (near Highway 20/26), and the Experimental Field Station

The low-volume air samplers are configured with particulate filters for collection of particulate radionuclides and charcoal filter cartridges for collection of ^{131}I. The samplers run continuously (24/7) and particulate filters are collected weekly and analyzed for gross-alpha and gross-beta activity. The filters are also composited quarterly (every 13 weeks) and analyzed for gamma-emitting radionuclides. Selected ESER sample composites are analyzed for ^{90}Sr, ^{137}Cs, and actinides (i.e., ^{238}Pu, $^{239/240}Pu$, and ^{241}Am) each quarter on a rotating basis. BEA screens for these radionuclides using gross-alpha/beta activity and gamma analyses, and requests additional radionuclide specific analyses if results are anomalous. The average flow rate of the samplers between weekly collections is approximately 3.38 m^3 hr^{-1} (2 ft^3 min^{-1}).

Tritium is also monitored in atmospheric water vapor at five locations (Blackfoot, Idaho Falls, Craters of the Moon, Van Buren Boulevard, and Atomic City). Samples of atmospheric water vapor are collected on average over a 27-day period, but vary from 14 days in the summer when the absolute humidity is high, to about 40 days in the winter when the absolute humidity is low. The average sampler flow rate is about 19.4 L hr^{-1} and the average absolute humidity in air at the INL Site is about 0.00345 g L^{-1}. Thus, about 43 mL of water is collected during a sampling period. From the collected atmospheric water sample, a 9 mL aliquot is taken and analyzed for tritium. The MDA for tritium in a 9 mL aliquot of collected water is 27.8 mBq (0.751 pCi).

METHODS

This section describes the frequency of detection methodology used to evaluate an air monitoring network. This includes a description of the atmospheric transport modeling and implementation and integration of the frequency of detection methodology with the atmospheric transport model output.

Frequency of Detection Methods

Frequency of detection is defined as the fraction of "events" that result in detection at either a single sampler or network of samplers. An "event" is defined as a release to the atmosphere of a specified amount of activity over a finite duration that begins on a given day and hour of the year. Assuming a single source is emitting radionuclides into the atmosphere, frequency of detection (*FD*) is defined as:

$$FD_{r,s} = \frac{\sum_{k=1}^{N} f\left(D_{r,s,k}\right)}{N} \tag{1}$$

where

$f(D_{r,s,k})$ = a binary function that returns 1 if the detection ($D_{r,s,k}$) is true (detection), and 0 if it is false (non-detection) for radionuclide r at sampler s, and event k,

N = the number of "events"

r = radionuclide index

s = sampler index

k = event index

The number of events is the number of release periods simulated in the assessment and depends on the number of hours of meteorological data present. For example, 8,761 hours of meteorological data are needed to model 8,760 1-hr events. Likewise, 8,784 hours of meteorological data are needed to model 8,760 24-hr events. A "detection" ($D_{r,s,k}$) is defined in terms of the radionuclide (r), the sampler (s), and the event (k). Detection is either true or false (i.e., either the sampler can detect the activity collected from airborne sampling or it does not). Detection is assigned a true value if the following condition is met:

$$TIC_{r,s,Q,Tr} \times F \geq MDA_r \quad (2)$$

where

$TIC_{r,s,Q,Tr}$ = time-integrated concentration of radionuclide r at sampler s for release quantity Q released over time Tr (Bq-hr m^{-3})

F = the sampler flow rate (m^3 hr^{-1})

MDA_r = minimum detectable activity for radionuclide r (Bq).

Equation (2) assumes background contribution is negligible. In practice, the activity accumulated on the filter would include activity released by the facility and any background contribution. Whether background is important will depend on the *TIC* necessary to produce in an inhalation dose of concern, and the background concentration of the radionuclide. In this application, background contributions were negligible.

Detections are a function of sampler performance (i.e., the flow rate and collection time), the sensitivity of the analytical techniques used to measure a given radionuclide, sampler placement relative source, and the meteorology during the release. The concentration is integrated over the time the sampler is operating (Ts) to obtain the total activity accumulated on the sampler filter.

The atmospheric transport model is used to compute the *TICs* at each of the samplers for a release of quantity Q released over a duration Tr, and sampling time of Ts. The time integrated concentration is defined by:

$$TIC_{r,s,Q,Tr} = \int_0^{Ts} C_{r,s,Q,Tr}(t)\,dt \tag{3}$$

where

$TIC_{r,s,Q,Tr}$ = time-integrated concentration for radionuclide *r* at sampler *s*, release quantity *Q*, release duration *Tr*, and sampling time *Ts* (Bq-hr m^{-3}).

$C_{r,s,Q,Tr}(t)$ = concentration as a function of time for radionuclide *r* at sampler *s*, release quantity *Q*, and release duration *Tr* (Bq m^{-3}).

The sampling time (*Ts*) is assumed to begin at the start of the release. This makes little difference in the results as long as the release duration is within the sampling period. For example, assume the sampling period begins on Monday at 8:00 AM and the sampling time is 168 hours (one week). An unplanned 1-hour release starts on Saturday at 8:00 AM and persists for 24 hours (i.e., ends Sunday at 8:00 AM). In this case, the total release is encompassed in the sampling period because the sampler filter is changed out on 8:00 AM the following Monday. This example assumes that the airborne plume from the release impacts the sampler (i.e., the plume travels in the direction of the sampler from the release point). The method may also be used to evaluate cases where the release begins a significant time into the sampling period and persists past filter change-out time.

As a matter of practicality, *TICs* are not calculated for each radionuclide and for all possible release durations. Instead, a *TIC* for a unit release (*TICu*) is calculated for each hour of the meteorological dataset. *TICu* is then scaled to the actual release quantity and duration to estimate the actual *TIC*. The *TICu* for a given source is defined by:

$$TICu_{s,h} = \frac{\int_h^{\infty} Cu_s(t)\,dt}{Qu} \tag{4}$$

where

$TICu_{s,,h}$ = time-integrated concentration at sampler *s* for a unit release rate from a given source that begins at hour *h* ($hr^2\ m^{-3}$)

$Cu_s(t)$ = concentration as a function of time at sampler *s* for a unit release rate from a given source beginning at hour *h* ($Bq\ m^{-3}$)

Qu = unit release rate from given source that persists for 1-hour ($1.0\ Bq\ hr^{-1}$).

It is important to note that the *TICu* values are defined for each source-sampler pair. In practice, infinity in the integrand is a finite amount of time to allow the activity emitted from the source over the 1-hour period to dissipate from the model domain. Complete dissipation occurs by either transport out of the model domain or dilution, resulting in concentrations that are negligible. The longest transport distance from any INL Site source to the edge of the model domain is about 180 km. A conservative estimate of the maximum transport time was made, assuming a mean wind speed of 1.0 m s^{-1} and a straight-line trajectory:

$$T = \frac{180\text{ km} \times 1000\text{ m/km}}{1.0\text{ m/s} \times 3600\text{ s/hr}} = 50\text{ hrs}.$$

Simulations were performed to confirm this value. If the integration time is long enough for complete dissipation, then the *TICu* value for 50 hours would be the same as the *TICu* value for 60 hours. Using 2006 meteorological data, it was found that in most cases a 50-hour integration time was sufficient for complete dissipation. However, there were some cases where the *TICu* value for 60-hours was slightly greater than that for 50-hours. This condition would occur during (1) very light wind speeds; (2) spatially variable wind directions, resulting in curvilinear trajectories; or (3) situations where the wind direction changed significantly during transport, resulting in recirculation of the airborne activity within the model domain. For this reason, the integration time was increased to 70-hours to assure *TICu* values captured all activity in the air observed at the sampler.

The *TICu* values are scaled and decay-corrected (to account for activity that decays on the filter) to obtain the *TIC* values for the actual release by the equation:

$$TIC_{r,s,Q,Tr} = \frac{\sum_{i=h}^{X+h} TICu_{s,i} e^{-\lambda_r (X+h-i)} \times Q_r}{Tr} \tag{5}$$

where

X = the minimum of *Tr* or *Ts*,

λ_r = radioactive decay constant (hr^{-1})

Q_r = release quantity for radionuclide *r* (Bq).

Equations 1 through 5 are used to evaluate the frequency of detection at a single sampler. The frequency of detection for the entire sampling network ($FDnet_r$) is evaluated by:

$$FDnet_r = \frac{\sum_{k=1}^{N} fn(D_{r,k})}{N} \tag{6}$$

where

$fn(D_{r,k})$ = a binary function that returns 1 if one or more samplers in the network has a detect, and 0 if no samplers in the network have a detect for radionuclide *r* and event *k*

N = the number of events.

The network *FD* is then the same if the release is detected by one sampler or multiple samplers. Thus, another quantity of interest called network intensity is defined. Network intensity is the fraction of samplers in the network that have positive detection. For example, if all detections from a release originate from a single sampler in the network, then the intensity will be low. However, if the release is detected by multiple samplers in the network, then the network intensity will be relatively high. Intensity is given by

$$I_r = \frac{\sum_{k=1}^{N}\sum_{s=1}^{Nw} f\left(D_{r,s,k}\right)}{N \times Nw} \qquad (7)$$

where

$f(D_{r,s,k})$ = a binary function that returns 1 if the detection ($D_{r,s,k}$) is true and 0 if it is false for radionuclide *r* at sampler *s*, and event *k*.

N = number of events

Nw = number of samplers in network.

Atmospheric Transport Model

This section describes the atmospheric transport model used to evaluate frequency of detection at the INL Site. The frequency of detection methodology does not depend on the atmospheric transport model, and any model appropriate to the modeling domain and meteorological and terrain conditions could be used.

Model Selection

Previous evaluations of air monitoring network designs have relied on steady-state Gaussian plume models to describe dispersion conditions during radioactive releases to the atmosphere (Pelletier 1968, Waite 1973, DOE 1991, NCRP 2010). Although these models may be appropriate for network planning, they have limited applicability for modeling the range of spatial and temporal scales necessary for evaluating network performance at the INL site. Thus, only non-steady-state Lagrangian puff dispersion models were considered for the regional analysis, although a Gaussian plume model could be considered for a local-scale analysis (<10 km). The three models considered were MDIFFH, HYSPLIT, and CALPUFF.

MDIFFH (Sagendorf et al. 2001) was developed by the Idaho Falls National Oceanic and Atmospheric Administration (NOAA) field office and was designed to estimate impacts over periods of up to one year or more on and around the INL Site, and is currently used to estimate annual dispersion factors from INL Site sources that are used to calculate representative individual and annual population doses. Although MDIFFH incorporates site-specific dispersion parameters and has been validated in the near field, it does not explicitly model terrain effects, utilize upper air data for vertical wind shear, include deposition and plume depletion, or allow discrete receptors (i.e., only receptors at grid nodes are allowed). The INL Site is situated on the relatively flat Eastern Snake River Plain and bordered by the Lemhi, Lost River, and Pioneer mountain ranges to the west, the Beaverhead and Centennial mountain ranges to the north, and the Big Hole and Caribou mountain ranges to the east. These features result in wind channeling between the ranges and influence diurnal air flow, resulting in spatially variable wind fields within the model domain. Although terrain effects are likely to be important because of the moderately complex terrain surrounding the INL Site, meteorological data collected by NOAA and used by MDIFFH implicitly incorporate these terrain effects into model simulations. Thus, the lack of discrete receptors was the most significant limitation of MDIFFH in terms of application to this study.

The HYSPLIT (Hybrid Single-Particle Lagrangian Integrated Trajectory) model was developed by the NOAA Air Resources Laboratory (Draxler 1999; Draxler et al. 2013) for emergency response modeling. The HYSPLIT model includes terrain effects (as resolved by the meteorological data), accounts for vertical wind shear, and includes deposition. Special gridded meteorological datasets covering the entire United States at various resolutions are used as basic input to the model. However, the model is not configured off-the-shelf for incorporating site-specific surface meteorological data as collected by NOAA.

The CALPUFF model (Scire et al. 2000a; Scire et al., 2000b) includes features and options that were considered important for this study. Namely, the model includes explicit treatment of terrain features; deposition and plume depletion; incorporation of upper air data (allowing for the effects of vertical wind shear to be modeled), and allows discrete receptors so the actual location of INL samplers are modeled instead of using the grid node nearest the sampler. CALPUFF is the U.S. Environmental Protection Agency (EPA)–approved, long-range (i.e., greater than 50 km) model for evaluation of air quality impacts in Federal Class 1 areas (i.e., national parks). For these reasons, CALPUFF was the model selected for this analysis. The EPA-approved version of the model (Version 5.8, Level 130731) was used in the calculations. The CALPUFF model code consists of three modules: (1) a meteorological model (CALMET), (2) a Lagrangian puff dispersion and deposition model (CALPUFF), and (3) a post-processing program (CALPOST). Numerous preprocessing programs are also used to develop input data sets. Computations were made using an eight-core MacPro workstation running OS X Lion. The FORTRAN source code was compiled using the gfortran (GNU Project) compiler for the Mac Unix operating system.

Model Domain and Grid

To adequately assess the INL Site ambient air monitoring network, the model domain must encompass the sampler locations, significant topographic features that influence airflow in the region, and primary population centers that may be impacted by INL Site releases. It was also desirable to include as many of the INL Site meteorological data stations as possible. Practical elements such as grid size and simulation run time were also considered (i.e., larger domains with finer grid resolution take longer to run).

The model domain selected (Fig. 1) is 240 km east to west and 200 km north to south for a total area of 48,000 km^2. This domain encompasses all sampler locations (with the exception of the sampler in Jackson, Wyoming) and all meteorological data stations that make up the INL Site Mesonet system (see Meteorological Data). It extends from the town of Carey in the west to the Idaho-Wyoming border in the east, and from 16 km south of Pocatello in the south to 20 km north of Dubois in the north. The eastern boundary includes the portion of Yellowstone National Park that lies just inside the Idaho State line.

The model domain was discretized into a uniform grid of 2-km resolution, comprising 120 east-west nodes and 100 north-south nodes for a total of 12,000 nodes. This grid resolution was selected to be consistent with the current MDIFFH model resolution of 2 km and to resolve the primary topographic features of the domain. Vertical discretization included 10 layers. Layer heights conformed to those recommended by EPA for federal land managers (Fox 2009). The top of each layer above ground level was set to 20, 40, 80, 160, 320, 640, 1200, 2000, 3000, and 4000 meters. The Universal Transverse Mercator (UTM) coordinate system was used in the model. The domain lies within UTM Zone 12.

Meteorological Data

Meteorological data included three years (2006-2008) of data from the prognostic Weather Research Forecasting (WRF) model (Skamarock et al., 2008), upper air data from Boise Idaho, surface data from 35 stations comprising the NOAA/INL Mesoscale Meteorological Monitoring Network (MESONET), and one airport surface station.

The WRF data consisted of 12-km data for 2006-2008 across the entire United States. These data were received from Alpine Geophysics LLC, Denver Colorado already processed through the CALWRF preprocessor. A subset of the data covering the model domain was extracted from the WRF files for use in CALMET. The WRF data contained wind speed, wind direction, temperature, precipitation, and atmospheric pressure at 37 levels above the ground surface.

Upper air data for 2006 through 2008 were obtained from the NOAA Earth Science Research Laboratory (ESRL) Radiosonde online database (NOAA, 2014a) for the Boise, Idaho Airport (Station Number 24141). Airport surface data for the Idaho Falls Regional Airport (Station Number 24145) were obtained from NOAA's National Centers for Environmental Information in the TD3505/CDO format (NOAA, 2014b).

Meteorological data from the NOAA/INL MESONET system (Fig. 3) was obtained from the NOAA Air Resources Laboratory Field Research Division in Idaho Falls, who maintains the network. Thirteen of the stations are located within the boundaries of the INL Site. The remaining stations are located at key locations on the Eastern Snake River Plain. Thirty of the stations are 15-m tall. Three of the stations on the INL Site extend to heights ranging from 46- to 76-m, with instrumentation installed at multiple levels, including at 15-m. Because of practical and aesthetic considerations, the measurements heights at Craters of the Moon and on Big Southern Butte stations are only 9-m and 6-m, respectively. Wind speed and direction at the 15-m level was used in all cases except for Craters of the Moon (9-m) and Big Southern Butte (6-m). Other data included temperature at the 2- and 15-m levels (when applicable) and height insensitive data including barometric pressure, relative humidity, and solar radiation. These data were converted to a format compatible with the SMERGE data preprocessor for use in CALMET.

Geophysical Data

Geophysical data include terrain elevations and land use. Land use defines surface roughness height, albedo, vegetative cover, and other parameters that determine energy balance at the earth's surface. The terrain model used United States Geological Survey (USGS) digital elevation model data. For the region encompassing the model domain, 22 one-degree digital elevation model data files were obtained (grid resolution of 90 m) from the USGS website (USGS 2014). Land use data were also obtained from the USGS website in the Global Lambert Azimuthal for North America format. Land use and land cover types are divided into 37 categories. Most of the land within the modeling domain is classified as rangeland. Forested land occupies the western, northern, and eastern boundaries of the domain, and agriculture land occupies regions near the I-15 and US 20 highway corridors.

CALPUFF/CALMET Model Options

Model options for the CALMET module were generally taken from those recommended by EPA for long-range transport as described in Fox (2009), with a few exceptions. A finer grid resolution of 2 km was used as opposed to the recommended value of 4 km because the modeling domain contained significant terrain features. The UTM coordinate system was also used instead of the Lambert Conic Conformal projection. The Lambert Conic Conformal projection is important for large domains (greater than 400 km), but is more cumbersome to work with when producing base maps with multiple geographic layers.

In general, default input parameters for CALPUFF were used, with two exceptions: (1) the terrain adjustment algorithm and (2) the dispersion coefficient option.

Terrain adjustment options in CALPUFF include the simple industrial source complex-type adjustment, the CALPUFF-type of terrain adjustment, and a partial plume path adjustment (default option). The CALPUFF-type terrain adjustment uses a simplified version of the complex terrain algorithm for subgrid features. In the CALPUFF-type terrain algorithm, properties of the puff are adjusted on the basis of local strain to the flow imparted by the underlying terrain. Based on analysis of isopleth plots of plumes in other simulations (Rood et al. 2008), the CALPUFF-type of terrain adjustment was used because it appeared to better simulate terrain effects.

The default dispersion coefficient option in CALPUFF is the Pasquill-Gifford Turner scheme (Dispersion Option 3) for urban and rural conditions. Other dispersion options include dispersion coefficients that are computed from micrometeorological variables and user input schemes. For these simulations, dispersion coefficients that are computed based on estimates of micrometeorological variables were chosen because they represent the current state-of-the-art in atmospheric dispersion modeling. This option calculates dispersion coefficients (σ_y and σ_z) based on an energy balance at the earth's surface. The energy balance is then related to turbulence using similarity theory.

Dispersion Patterns

An isopleth map of the annual unit *TIC* values for steady-state releases from the 70-m TRA-770 stack is illustrated in Fig. 3. In general, air flow is channeled up and down the Eastern Snake River Plain in a diurnal cycle. Drainage flow from northeast to southwest down the Plain occurs in the evening hours as cooler air sinks and descends off the higher terrain to the west and north of the INL Site. During daytime hours winds are primarily out of the southwest owing to predominate westerly winds and diurnal surface heating. Local terrain effects are evident along the mountains to the northwest and southeast of the INL Site. Additionally, the elevated plume impacts the upper reaches of one of the buttes south of the INL Site boundary and where the meteorological station labeled SUM is located. Dilution and dispersion result in a factor of 15 to 30 reduction in ambient air concentration from the INL Site to the surrounding communities in Idaho Falls and Pocatello.

Implementation of Frequency of Detection Methods

Although a three-year meteorological data set was processed, only one year of data (2006) was used for frequency of detection analysis. Development of *TICu* values for each source for one year of data took about 12-14 hours of simulation time per emission source. Analysis of model output using all three years of data showed that annual *TICu* values at each of the samplers were relatively consistent from year-to-year. Thus using a different year or more than one year of meteorological data was not expected to make a significant difference in the frequency of detection results.

Frequency of detection calculations were implemented using Fortran codes and Perl scripts. A Perl script was used as a "wrapper" to set-up, execute, and post-process the CALPUFF simulations for calculating *TICu* values. The script takes the years, days, and hours that will be simulated and the source location and release parameters as input. The script then constructs a run matrix that includes (1) selecting the CALMET files that cover the meteorological period simulated, (2) writing the CALPUFF input files and executing CALPUFF, (3) post-processing results at the sampler locations using CALPOST and calculating the *TICu*, and (4) writing *TICu* to an output file. The *TICu* file is not model dependent, and could be developed using any atmospheric transport model. For example, a Gaussian Plume model was also developed to calculate *TICu* values for near-field samplers located within several kilometers of selected sources.

A Fortran code was used to calculate frequency of detection. The code reads the *TICu* results generated from the atmospheric transport model, and a parameter file that identifies all samplers in the simulation, sampler flow rates, radionuclide detection limits and release quantities, and whether to include the sampler in the analysis. Output includes frequency of detection results for individual samplers and the sampling network, network intensity, probability distributions of estimated *TICs* and doses for a given release duration, and maximum *TICs* and doses for each radionuclide and source.

Emission Sources

Eleven INL emission sources were considered in the assessment (Table 1). Sources included three stack sources located at the ATR Complex, INTEC and MFC facilities, and ground-level releases at all major facilities. Where a specific emission source was not identified, ground sources were located near the center of each facility and assumed an initial σ_y of 100-m and initial σ_z of 20 m to account for wake effects and multiple emission points. Frequency of detection results were calculated separately for each of the emission sources. The ability of a monitoring network to detect a radionuclide release depends on the detection limit of the radionuclide in the sample, the quantity of the radionuclide released, the duration of the release, and the sampler flow rate. To evaluate the effectiveness of an air monitoring network, minimum relevant release quantities must be determined. A minimum relevant release quantity is the minimum quantity of a radionuclide released from a facility that would result in a given dose constraint being met at a defined receptor.

Important Radionuclides and Relevant Release Quantities

Release of radionuclides to the environment are regulated by limits on the total effective dose incurred by members of the public exposed to radionuclides present in the environment that are attributed to releases from the facility. Department of Energy regulations limit the total effective dose to a member of the public from radiological activities including releases to the environment to 1 mSv yr^{-1} (DOE 2011a). The effective dose limit for members of the public exposed to radionuclides released to the atmosphere from DOE facilities is 0.1 mSv yr^{-1} (EPA, 2006). To ensure detection of radionuclides well before dose standards are approached, thus assuring protection of the public, a more conservative monitoring and modeling dose constraint of 10% of 0.1 mSv yr^{-1} limit (0.01 mSv yr^{-1}) to a member of the general public was adopted. Thus, a minimum relevant release quantity would be the activity released from a facility that has the potential to result in a dose of 0.01 mSv yr^{-1} to a member of the public. Because particulate air samplers only collect for seven days before the filter change-out, it would be important for the monitoring network to detect a release during the 1-week sampling time that would have the potential, if continued over the course of a year, to produce an estimated dose to a member of the public of 0.01 mSv yr^{-1}. Thus, the minimum release quantity that results in a dose of 1.9×10^{-4} mSv (0.01 mSv yr^{-1} ÷ 52 weeks yr^{-1}) over a 1-week period to a member of the public was defined as the minimum relevant release quantity.

Demonstration of compliance with the 0.1 mSv yr^{-1} dose criteria at the INL Site is documented in the Annual Site Environmental Report (ASER). The ASER contains monitoring results and public dose estimates based on estimated effluent releases, atmospheric transport modeling, terrestrial transport modeling, and receptor scenarios for residents living near the INL Site boundary (DOE-ID 2014). Important radionuclides released from INL facilities identified through ASER modeling and that are routinely monitored for include ^{241}Am, ^{137}Cs, ^{238}Pu, ^{239}Pu, and ^{90}Sr. Tritium was also identified as an important radionuclide, but is not sampled or measured in the same manner as the particulate radionuclides. Furthermore, tritium is only released from three of the major INL Site facilities; RWMC, INTEC (CPP-1774 stack), and ATR Complex (TRA-770 stack).

Calculated doses are based not only on direct inhalation, but other exposure pathways from air emissions as well, using a unit all-pathway dose factor (mSv Bq^{-1}) calculated from the ASER model output for calendar year 2013. These pathways include ingestion of meat, milk, and produce, cloud shine, and external exposure from radionuclides deposited on soil. The ASER all-pathway unit dose factor, breathing rate, and air monitor sampling time were used to estimate the minimum relevant release quantity that would result in the dose constraint being met at any of the public receptors. The release quantity is calculated using the following equation

$$Qr = \min\left[\frac{D_{ED}Tr}{\sum_{i=h}^{Tr+h} TICu_{p,i}\, e^{-\lambda_r (X+h-i)}\, UDF\, BR}\; p = 1\ldots n\right] \qquad (8)$$

where

Qr = minimum relevant release quantity that results in an effective dose, D_{ED} (Bq),

D_{ED} = the effective dose constraint (1.9×10^{-4} mSv),

Tr = release duration (168 hours),

h = hour index (1–8760),

$TICu_{p,i}$ = unit *TIC* value for public receptor *p* and hour *i* (hr^2 m^{-3}),

UDF = all-pathway unit dose factor (mSv Bq^{-1}),

BR = ASER breathing rate for reference individual (0.917 m^3 hr^{-1}),

n = number of public receptors,

p = public receptor index.

Note that in *TICu*, the public receptor index (*p*) replaces the sampler index (*s*). For conservatism, ASER uses the inhalation solubility class with the highest dose coefficient except for tritium, where the chemical form is tritiated water vapor. For particulate samplers, frequency of detection was based on a release duration and sampling time of 168 hours (1 week). For tritium, frequency of detection was based on a release time of 168 hours and a sampling time of 648 hours (27 days). The release duration can be any increment of time greater than or equal to the meteorological sampling time (1-hour).

The all-pathway unit dose factors were calculated using the total dose reported in the 2013 ASER report at the location of the maximally exposed individual (MEI), the ASER air concentration at that location, and the breathing rate.

$$UDF = \frac{D_{MEI}}{C_{MEI} BR} \tag{9}$$

where

D_{MEI} = annual all-pathway effective dose at the MEI location (mSv yr^{-1}),

C_{MEI} = annual average air concentration at the MEI location (Bq m^{-3}),

BR = annual breathing rate (8033 m^3 yr^{-1}).

Other criteria may be used as well depending on monitoring objectives. Using the all-pathway unit dose factors to determine minimum relevant release quantities results in the smallest amount of activity released that has the potential for a dose of regulatory significance. Thus, if the monitoring network can detect the minimum release quantity, it will certainly have the ability to detect larger release quantities. The all-pathway unit dose factors along with the inhalation dose coefficients from DOE (DOE 2011b), and analytical MDA are presented in Table 2. Note that the inhalation dose coefficient for the actinides is only slightly less than the all-pathway unit dose factors, while for the fission and activation products, the difference is more pronounced. This is because for actinides, most of the dose is incurred through direct inhalation, while for the fission and activation products, a significant portion of the dose is incurred through ingestion pathways and external radiation. Relevant release quantities for the important radionuclides and the INL sources are presented in Table 3.

Model Validation

Atmospheric dispersion models are inherently uncertain, and model validation exercises provide a means to quantify the magnitude of uncertainty and build confidence in the model. Radonjic et al. (2005) used CALPUFF to model short-term releases of fission and activation products from INL Site sources. The CALPUFF model was validated as part of this project using data from a 1999 atmospheric SF_6 tracer experiment conducted by NOAA (Clawson et al., 2000). The tracer dataset consisted of hourly measurements of SF_6 at 56 samplers distributed in sampling arcs 15-, 30-, and 50-km from the source. Seven separate tests were conducted under varying meteorological conditions, and in general 59% of model predicted maximum hourly-average concentrations were within a factor of two of the observations.

Rood (2014) evaluated CALPUFF for one- and 9-hour average concentrations using a separate SF_6 tracer study performed at the former U.S. DOE Rocky Flats Plant. Twelve, 11-hour tests were conducted where a SF_6 tracer was released and measured hourly at 140 samplers distributed in concentric rings 8- and 16-km from the release point. Results of the Rood (2014) study showed CALPUFF exhibited little bias when estimating the maximum 1-hour average concentration (geometric mean predicted-to-observed ratio of 0.99) and over 50% of the predictions were within a factor of two of the observations.

Another model validation exercise was performed by the authors using annual-average predicted and observed concentrations at 21 air samplers from a 587-GBq (15.9-Ci) release of ^{125}Sb from the Flourinel and Storage (FAST) stack at the INTEC facility in 1987. The 21 samplers were located both on and off the INL Site. Shorter-term averages (i.e., weekly or monthly) would have been more appropriate but were not available. Nevertheless, the annual average comparison provides a measure of model performance within the entire model domain using the INL Site sampling network. The release of ^{125}Sb in 1987 was identified in a 1987 DOE-ID memo* as an opportunity to validate the MESODIF (Start and Wendell 1974) meteorological air dispersion model. The MESODIF model was the precursor to the MDIFFH model described previously. Annual average concentrations were compared with MESODIF model-predicted values in a DOE memo†. The MESODIF simulation was based on annual average dispersion conditions for 1987 and a constant release of the ^{125}Sb activity over the year. The CALPUFF simulation was based on monthly-average dispersion conditions and monthly release rates of ^{125}Sb as provided in DOE-ID (1988). Releases varied considerably from month to month, ranging from 170 GBq (4.59 Ci) for February to 0.07 GBq (0.0019 Ci) for November, 1987 (Table 4). Because meteorology and dispersion conditions are generally repeatable from year-to-year, the 3-year meteorological dataset was used in CALPUFF (i.e., 2006, 2007, and 2008) to estimate average monthly dispersion conditions for 1987.

Performance measures included the fraction bias (*FB*), normalized mean square error (*NMSE*), regression coefficient (Hanna et al., 1991), and geometric mean and standard deviation of the predicted-to-observed ratios. Fractional bias is given by

$$FB = \frac{2(\overline{C}_o - \overline{C}_p)}{\overline{C}_o + \overline{C}_p} \tag{10}$$

where C_p and C_o are the predicted and observed concentrations, respectively. Overbars indicate averages over the sample. The *NMSE* is given by

$$NMSE = \frac{\overline{(C_o - C_p)^2}}{\overline{C}_o \, \overline{C}_p} \tag{11}$$

Log-transformed measures include the geometric mean bias (*MG*) and the geometric mean variance (*VG*) and are defined by

$$MG = \exp\left(\overline{\ln C_o} - \overline{\ln C_p}\right) \quad (12)$$

$$VG = \exp\left[\overline{\left(\ln C_o - \ln C_p\right)^2}\right] \quad (13)$$

where the overbars indicate averages over the sample. Geometric mean bias values of 0.5 and 2.0 indicate a factor of 2 over-prediction and under-prediction, respectively. A *VG* value of 1.6 indicates a typical factor of about 2 between the predicted and observed data pairs. A perfect model would have *FB* and *NMSE* values of 0, and *MG* and *VG* values of 1.0.

Annual-average predicted and observed ^{125}Sb concentrations in air at the samplers are presented in Table 5. The geometric mean of the predicted-to-observed ratio for CALPUFF and MESODIF was 0.73 and 2.17, respectively, and the geometric standard deviation for CALPUFF and MESODIF was 2.22 and 3.22, respectively (Table 6). The log-transformed regression coefficient (*r*) was 0.853 for CALPUFF and 0.739 for MESODIF (Fig. 4). An *F*-test indicated that the linear regression for both CALPUFF and MESODIF were significant (P>0.95). The other performance measures are summarized in Table 6. By almost all other quantitative measures of performance, CALPUFF was judged to perform better than MESODIF. The NMSE for CALPUFF was substantially higher (although not significantly different) than its optimum value, and was driven almost entirely by the highest predicted (9620 MBq m^{-3}) and observed (3590 MBq m^{-3}) concentration at the BEA-INTEC sampler. This validation exercise demonstrates that CALPUFF provides concentration estimates from INL Site releases that were within the established uncertainty of atmospheric transport models for predicting annual average concentrations in a complex-terrain environment (Miller and Hively 1987).

RESULTS AND DISCUSSION

Frequency of detection and network intensity results for the minimum relevant release quantities for each major INL facility including the three stack sources are presented in Table 7. All detection frequencies for 168-hr release durations exceed 97.5% for all sources, radionuclides, release times. Network intensity results for particulates ranged from 3.75% for ^{241}Am releases from MFC-1774 to 62.7% for ^{90}Sr released from the NRF facility. Despite having only four samplers, detection frequency and network intensity for tritium was excellent.

For particulate releases, it is assumed the entire 168-hour release is captured during the 168-hour sampling time (tritium uses a 648-hr sampling time). This of course is an ideal situation, and in most cases, the release will have started sometime during the sampling period, so a portion of the release will be captured during the week the release began, and the remainder of the release will be captured on the subsequent week. The effects of simulating week-long releases beginning partway through 1-week sampling period are illustrated in Fig. 5 for a 0.029 GBq ^{241}Am releases from the TRA-770 stack. If the release begins during the latter stages of the first week sampling period such that only a few hours of the release are encompassed the first sampling period, then most of the release will be captured during the second week. Minimum detection frequencies occur when the release starts midway through the sampling period. In this example, frequency of detection reaches a minimum of about 75% for a release starting 84 hours into the first week sampling period.

The sensitivity of detection frequency to release time for a fixed release quantity is illustrated in Fig. 6. The same quantity released over a shorter time will result in higher concentrations, but a smaller spatial extent of the plume, thereby lowering the probability that the plume will impact a sampler. The minimum network detection frequency was 3.85% for a 0.029 GBq release of ^{241}Am from the TRA-770 stack released over 1-hour period. For a 1-hr 0.98 GBq release of ^{90}Sr from the same source, the detection frequency was 69.9%. The difference between the ^{241}Am and ^{90}Sr detection frequencies are related to the minimum relevant release quantities that yield a 1-week effective dose of 0.00019 mSv. While the MDA for ^{90}Sr is about a factor of 8 greater than that of ^{241}Am, the release quantity of ^{90}Sr was a factor of 33.8 greater than ^{241}Am. The net effect is that more ^{90}Sr activity above the MDA is collected on the filter compared to ^{241}Am, resulting in a greater detection frequency of ^{90}Sr compared to ^{241}Am.

Assuming a frequency of detection performance standard for the network of 95% for a 168-hr release, the existing INL network would meet such a standard. However, the question remains of whether the sampling network in its current configuration is optimal. That is, can the performance and efficiency of the network be improved by adding, removing, or repositioning samplers? Examination of individual sampler detection frequencies can provide valuable insight in terms of their overall effectiveness within the network (Table 8). Limiting the examination to only onsite samplers, we note that some samplers have generally low detection frequencies or when detection frequency is high, there are other samplers located nearby that have similar detection frequencies. Also note that only a few samplers had detections for sources at MFC. This is reflected in the relatively low network intensities for this source. Frequency of detection methods can be used to identify optimum placement and number of samplers and is discussed in the next section.

Network Optimization

The frequency of detection method can be useful for identifying optimum sampler locations and removing samplers that are ineffective. This procedure can be used to design a sampling network or to evaluate an existing network. The procedure is iterative, and begins with identifying all potential or existing sampler locations and running the simulation for the release quantity of interest. Next, individual samplers that have high detection frequencies and are in different azimuth locations are identified, along with poor performing samplers. The model is rerun using a selected set of samplers having high detection frequencies and spaced apart so as to improve the likelihood of detection of a plume traveling in multiple directions from the source. Frequency of detection is then calculated and the overall network detection frequency is compared to the original sampler configuration, and adjustments are made to optimize network performance. A sample application of network optimization was performed for the existing INL Site network. In this example, hypothetical samplers were added south of the RWMC, and north and south and of MFC to improve detection frequency and intensity for releases from MFC and RWMC sources. At the same time, samplers BEA-ARA, BEA-PBF, ESER-MAI, and ESER-FAA were removed from the network because these samplers either had poor performance or were located near other samplers that exhibited similar performance. Network detection frequency remained greater than 97% for all sources and all radionuclides despite the removal of four samplers. Network intensity decreased an average of 4.7% across all sources except MFC sources, mainly due to the removal of the BEA-ARA, and BEA-PBF samplers. For MFC sources, network intensity improved from 5.05% to 10.6% for ^{241}Am releases from MFC-764, and from 3.75% to 8.8% for ^{241}Am releases from MFC-774. Similar improvements in network intensity from MFC sources were observed for ^{239}Pu and ^{238}Pu as well, while a smaller improvement in intensity was observed for ^{137}Cs and ^{90}Sr. Sources that exhibited a decrease in intensity already had relatively high network intensities ranging from 11.3% for ^{241}Am releases from CPP-708 to 62.7% for ^{90}Sr releases from the NRF. Thus, overall network performance and efficiency could be improved by simply moving some samplers to optimum locations, and removing samplers that showed similar performance to other existing samplers.

Of course, other considerations such as available power or access may limit placement of samplers, or they may justify sampler placement in locations that are less than optimal, such as requirements to be near population centers or National Monuments. In these cases, frequency of detection methods could also be used to assess the adequacy of the sampler in terms of detecting releases that have dose consequences at those locations. Additionally, frequency of detection methods could be used to test the likelihood that a background sampler will detect releases from a potential source.

CONCLUSIONS

The frequency of detection methodology is a useful and effective approach for quantitative evaluation of an air monitoring network. The methodology was demonstrated by performing an assessment of the INL Site ambient air monitoring network. Based on this assessment, the current INL monitoring network is more than adequate (greater than 95% detection frequency for a 168-hr release) in terms of detecting a minimum relevant release that would result in a weekly dose of 1.9×10^{-4} mSv, or if continuous over a year, 0.01 mSv (10% of the annual dose limit of 0.1 mSv from airborne releases). However, improvements in network performance were identified using the methodology.

While a wind rose or annual average dispersion modeling may serve as a first cut at identifying sampler locations, it cannot quantify the ability of the network to detect releases. Furthermore, many releases at nuclear facilities are not constant throughout the year. The frequency of detection methodology allows for evaluation of short-term releases that include effects of short-term variability in meteorological conditions. As presented, the methodology is not tied to any specific dispersion model, and in fact, a Gaussian Plume or other model could be used as well. For this exercise, the size of the modeling domain dictated the use of a Lagrangian puff model because of spatially-variable meteorological conditions and terrain that typically occur across regions of this size. For smaller domains or near-field network designs, a Gaussian Plume model may be perfectly adequate.

The detection frequencies provided in this paper assume a negligible background contribution. However, depending on the levels of background, the activity accumulated on the filter that would provide a positive detection could be indistinguishable from the activity accumulated on the filter from background. The effects of background concentrations on the ability of the sampling network to detect releases can be evaluated using this methodology by adjusting the MDA to reflect background contributions.

Application of the methodology should include input from stakeholders (i.e., regulators, operators, and members of the public), who would need to come to consensus on the acceptable frequency of detection level (i.e., 90%, 95%, 97.5%, etc.) and dose constraints that would be adhered to. Facility operators and technical staff would also need to provide input on the practical physical constraints of any sampling program including sampler flow rates, sampling times, radionuclide MDAs, and availability of electrical power and access at a given location.

Acknowledgments

The authors wish to thank Scott Lee of Battelle Energy Alliance and Betsy Holmes, DOE Idaho for their overall support of this work.

REFERENCES

Clawson, K. L., J. F. Sagendorf and R. G. Carter. Comparisons of a puff trajectory model with real time tracer measurements. Preprint, 11th Joint Conference on the Applications of Air Pollution Meteorology with the Air & Waste Management Association, January 9-14, 2000, Long Beach, California, American Meteorological Society, pp. 293-298 2000.

DOE (U.S. Department of Energy). Environmental regulatory guide for radiological effluent monitoring and environmental surveillance. DOE/EH-0173T; January 1991.

DOE. DOE Order 458.1, Radiation protection of the public and environment; February 2011a.

DOE. Derived concentration technical standard. Department of Energy Standard, DOE-STD-1196-2011; April 2011b.

DOE-ID (U.S. Department of Energy, Idaho Operations Office). Radioactive waste management information for 1987 and record to date. DOE/ID-10054(87), U.S. Department of Energy, Idaho Operations Office, Idaho Falls, ID; 1988.

DOE-ID. Idaho National Laboratory Site Environmental Report Calendar Year 2013. DOE/ID-12082(13). U.S. Department of Energy, Idaho Operations Office, Idaho Falls, ID; 2014.

Draxler, R.R. HYSPLIT-4 user's guide. NOAA Technical Memorandum, ERL ARL-230. National Oceanic and Atmospheric Administration, College Park, Maryland; 1999.

Draxler, R.R., B Stunder, G. Rolph, A. Stein, and A. Taylor. HYSPLIT4 User's Guide, Version 4 revision April 2013, Available at http://ready.arl.noaa.gov/HYSPLIT.php, National Oceanic and Atmospheric Administration, College Park, Maryland; 2013.

EPA (U.S. Environmental Protection Agency). 40 CFR 61, Subpart H. National emission standards for emissions of radionuclides other than radon from Department of Energy facilities. 40 CFR Part 61 Subpart H; July 2006.

Fox, T.J. Clarification on EPA-FLM recommended settings for CALMET. Memorandum from Tyler J. Fox to Regional Modeling Contacts. U.S. Environmental Protection Agency, Research Triangle Park, North Carolina; August 31, 2009.

Hanna S.R., D.G. Strimaitis, and J.C. Chang. Hazard response modeling uncertainty (a quantitative method), volume 1: User's guide for software for evaluating hazardous gas dispersion models. Florida: Air Force Engineering and Service Center, Tyndall Air Force Base; 1991.

Miller, C.W. and L.M. Hively. A Review of Validation Studies for the Gaussian plume Atmospheric Dispersion Model. Nuclear Safety 20(4): 522–531; 1987.

Pelletier, C.A. Performance and design of an environmental survey. In: Health Physics Society symposium proceedings, environmental surveillance in the vicinity of Nuclear Facilities, ed. W.C. Reinig, Charles C. Thomas, publisher, LC number 69-12987; 1968.

NCRP (National Council of Radiation Protection). Design of effective radiological effluent monitoring and environmental surveillance programs. Report 169. National Council on Radiation Protection, Bethesda, Maryland; 2010.

NOAA (National Oceanic and Atmospheric Administration). Earth Science Research Laboratory (ESRL) Radiosonde online database. Available at http://esrl.noaa.gov/raobs/, Accessed August, 2014a.

NOAA. National Centers for Environmental Information. Available at http://www.ncdc.noaa.gov, Accessed August, 2014b.

Radonjic, A, R. Stager, and A.I. Apostoaei. An analysis of atmospheric dispersion of radionuclides released from the Idaho Chemical Processing Plant (ICPP) (1957-1959). Senes Consultants, Richmond Hill, Ontario Canada; 2005.

Ritter, P.D., C.A. Whitaker, W.J. Behymer, and J.F. Sagendorf. Evaluation of the Response of the INEEL Radiological Air Surveillance Network to Acute and Chronic Releases. In: J.M. Barnett, G.A. Vasquez, W.E. Hughes, and S.V. Anderson eds. NESHAP Annual Meeting on Radioactive Air Ten Year Retrospective, 2002-2011. PNNL-SA-98876; December, 2013.

Rood A.S., P.G. Voillequé, S.K. Rope, H.A. Grogan, and J.E. Till. Reconstruction of atmospheric concentrations and deposition of uranium and decay products released from the former uranium mill at Uravan Colorado USA. Journal of Environmental Radioactivity, 99: 1258–1278; 2008.

Rood, A.S. Performance evaluation of AERMOD, CALPUFF and legacy air dispersion models using the Winter Validation Tracer Study dataset. Atmospheric Environment, 89: 707–720; 2014

Sagendorf, J.F., R.G. Carter, and K.L. Clawson. MDIFF transport and diffusion models, NOAA Technical Memorandum OAR ARL-238, National Oceanic and Atmospheric Administration; February 2001.

Scire, J.S., D.G. Strimaitis, and R.J. Yamartino. A user's guide for the CALPUFF dispersion model version 5. Earth Tech Inc., Concord, Massachusetts; 2000a.

Scire, J.S., F.R. Robe, M.E. Fernau, and R.J. Yamartino. A User's Guide for the CALMET Meteorological Model Version 5. Earth Tech Inc., Concord, Massachusetts; 2000b.

Skamarock, W.C., J.B. Klemp, J. Dudia, D.O. Gill, D.M. Barker, M.J. Duda, X. Huang, W. Wang, and J.G. Powers. A description of the advanced research WRF version 3. NCAR/TN-475+STR, National Center for Atmospheric Research, Boulder Colorado (http://www.wrf-model.org); 2008.

Start, G.E. and L.L. Wendell, 1974, Regional effluent dispersion calculations considering spatial and temporal meteorological variations, NOAA Tech Memo, ERL ARL-44; 1974.

USGS (United States Geological Survey). EROS Data Center for digital data Available at (http://edc.usgs.gov/products/elevation/dem.html)., Accessed August, 2014.

Waite, D.A., 1973, *An Analytical Technique for Distributing Air Sampling Locations Around Nuclear Facilities*, BNLW-SA-4534, May 1973.

Footnotes

* Memorandum from E.W. Chew, Chief Environmental Science Branch, Radiological and Environmental Sciences Laboratory, to M.M. Williamson, Director Radiological and Environmental Sciences Laboratory, U.S. Department of Energy, Idaho Operations Office, May 13, 1987.

† Letter to L.E. Rockhold, Battelle Energy Alliance LLC from R.L. Dickson, U.S. Department of Energy, Idaho Operations Office, March 7, 2012.

Figure Captions

Fig. 1. Eastern Idaho model domain showing major cities, Idaho National Laboratory Site boundary, terrain elevations, and air monitoring locations (triangles). The station labeled FRENCHCBN is not a monitoring station but the location of the Maximally Exposed Individual for annual dose assessment modeling.

Fig. 2. Major facilities on the INL and locations of potential nearby residences (circles). Some locations represent more than one potential residence and not all locations are currently habitated.

Fig. 3. INL MESONET meteorological tower locations (circles with cross) and isopleths of annual unit time-integrated concentration values ($hr^2\ m^{-3} \times 10^9$) for releases from the TRA-770 stack.

Fig. 4. Predicted and observed annual average ambient air concentrations of ^{125}Sb for 1987.

Fig. 5. Frequency of detection as a function of first-week sampling time for a 168-hr release split between two weeks. For example, a release that begins at hour 108 during the first week sampling period will have 60 hours of sampling time during the first week and 108 hours of sampling time during the second week. Plot is based on frequency of detection of a 0.029 GBq release of ^{241}Am from the TRA-770 stack.

Fig. 6. Sensitivity of detection frequency as a function of release time for 0.029 GBq release of ^{241}Am and a 0.98 GBq release of ^{90}Sr from the TRA-770 stack.

Table 1. Modeled source locations for the frequency of detection evaluation.

Facility	Source	Release type	Source description
ATRC	TRA-770	Stack	Advanced Test Reactor Complex, Advanced Test Reactor Stack
INTEC	CPP-708	Stack	Idaho Nuclear Technology and Engineering Center, Main Stack
MFC	MFC-764	Stack	Materials Fuels Complex, Experimental Breeder Reactor-II Main Stack
ATRC	ATR	Ground	Advanced Test Reactor Complex, no specific source identified, release assumed from center of facility
CFA	CFA-625	Ground	Central Facilities Area, lab fume hoods (near center of CFA)
CITRC	PBF-632	Ground	Critical Infrastructure Test Range Complex, Waste Reduction Operations Complex Support Building Vent
INTEC	CPP-1774	Ground	Idaho Nuclear Technology and Engineering Center, Three Mile Island-2 Spent Fuel Storage Installation (Near center of INTEC)
MFC	MFC-774	Ground	Materials and Fuels Complex, Zero Power Physics Reactor Support Wing
NRF	NRF	Ground	Naval Reactors Facility, no specific source identified, release assumed from center of facility
RWMC	RWMC	Ground	Radioactive Waste Management Complex, no specific source identified, release assumed from center of facility
SMC/TAN	TAN-679	Ground	Specific Manufacturing Capability/Test Area North, Manufacturing and Assembly Building

Table 2. All-pathway unit dose factors, inhalation effective dose coefficients from DOE (2011b), and minimum detectable activity in airborne samples for important radionuclides at the INL Site.

Radionuclide (Solubility Class)	All-pathway unit dose factor ($\mu Sv\ Bq^{-1}$)	Reference person inhalation dose coefficient ($\mu Sv\ Bq^{-1}$)	Minimum detectable activity [MDA] (mBq)
^{241}Am (F)	101	98.1	1.07
^{137}Cs (S)	1.16	0.42	25.9
^{238}Pu (F)	113	110	0.814
^{239}Pu (F)	125	121	0.814
^{90}Sr (S)	3.30	0.16	7.96
^{3}H (V, HTO)	2.40×10^{-4}	1.93×10^{-5}	27.8

Table 3. Minimum relevant release quantities (GBq) for each source that result in a 1-week dose of 0.00019 mSv at an offsite resident location.

Source	^{241}Am	^{137}Cs	^{238}Pu	^{239}Pu	^{90}Sr	^{3}H
ATR	0.043	3.8	0.039	0.035	1.5	
CFA-625	0.024	2.1	0.021	0.019	0.79	
CITRC	0.026	2.3	0.023	0.021	0.87	
CPP-1774	0.038	3.3	0.034	0.031	1.3	15,940
CPP-708 (stack)	0.035	3.1	0.032	0.029	1.2	
MFC-764 (stack)	0.12	10.4	0.11	0.10	4.0	
MFC-774	0.012	1.02	0.010	0.010	0.39	
NRF	0.062	5.4	0.055	0.050	2.1	
RWMC	0.016	1.4	0.014	0.013	0.53	6,686
TAN-679	0.022	1.9	0.020	0.018	0.74	
TRA-770 (stack)	0.029	2.6	0.026	0.024	0.98	12,395

Table 4. Monthly estimates of 1987 ^{125}Sb releases from FAST stack at INTEC facility.

	^{125}Sb Release (GBq)	^{125}Sb Release (Ci)
January	28.1	0.759
February	170	4.59
March	53.7	1.45
April	55.4	1.50
May	35.4	0.956
June	42.9	1.16
July	34.7	0.938
August	54.8	1.48
September	88.8	2.40
October	20.4	0.550
November	0.070	0.0019
December	2.68	0.072
Total	587	15.9

Table 5. Predicted and observed ^{125}Sb concentrations at INL network air samplers

Location	Sampler designation	MESODIF ($\mu Bq\ m^{-3}$)	CALPUFF ($\mu Bq\ m^{-3}$)	Measured ($\mu Bq\ m^{-3}$)
Craters of the Moon NM	ESER-CRA	15.5	14.3	81.4
Idaho Falls	ESER-IDA	23.3	20.5	37.0
Arco	ESER-ARC	19.2	33.4	96.2
Atomic City	ESER-ATO	501	83.0	81.4
FAA Tower	ESER-FAA	154	42.0	7.40
Howe	ESER-HOW	154	101	177
Monteview	ESER-MON	77.3	54.7	29.6
Mud Lake/Terreton	ESER-TER	270	78.3	88.8
RENO	[a]	77.3	62.8	70.3
Materials Fuel Complex	BEA-MFC	386	76.6	88.8
Auxiliary Reactor Area	BEA-ARA	618	95.1	111
Central Facilities Area	BEA-CFA	3,087	542	629
Experimental Breeder Reactor	BEA-EBR	1,158	381	1,073
Experimental Field Station	BEA-EFS	3,087	696	592
Idaho Nuclear Technology and Engineering Center	BEA-INTEC[b]	3,859	9,624	3,589
Naval Reactors Facility	BEA-NRF	1,544	162	218
Power Burst Facility	BEA-PBF	1,544	155	414
Radioactive Waste Management Complex	BEA-RWMC	772	261	592
Test Area North	BEA-SMC	309	92.2	59.2
Advanced Test Reactor Complex	BEA-TRA[c]	1,544	232	629
Van Buren Boulevard	BEA-VANB	1,930	524	1,184

a. Inactive station formally located 11 km southeast of the ESER-BLU station.

b. Formerly Idaho Chemical Processing Plant.

c. Formerly Test Reactor Area

Table 6. Performance measures for the ^{125}Sb comparison with CALPUFF and MESODIF.

Performance Measure	Optimum Value	CALPUFF[a]	MESODIF[a]
Fractional Bias (*FB*)	0.0	**–0.297**	–0.728
Normalized Mean Square Error (*NMSE*)	0.0	**6.05**	**1.76**
% within a factor of 2	100	52.4	33.3
Geometric Mean Bias (*MG*)	1.0	**1.36**	0.460
Geometric Mean Variance (*VG*)	1.0	**2.02**	6.73
Geometric Mean P/O ratio (*GM*)	1.0	0.73	2.17
Geometric Standard Deviation (*GSD*)	1.0	2.22	3.22
Regression Coefficient (*r*)	1.0	**0.929**	0.758
Regression Coefficient, log-transformed	1.0	**0.853**	0.739

[a.] Bolded values indicate 95% confidence intervals calculated with the BOOT software (Hanna et al. 1991) encompassed the optimum value of the performance measure.

Table 7. Frequency of detection and intensity results for a 168-hr release of the minimum relevant release quantity that would result in a 1-week dose of 0.00019 mSv.

Frequency of Detection						
Source	^{241}Am	^{137}Cs	^{3}H	^{238}Pu	^{239}Pu	^{90}Sr
ATR	100%	100%		100%	100%	100%
CFA-625	100%	100%		100%	100%	100%
CITRC	100%	100%		100%	100%	100%
CPP-1774	100%	100%	100%	100%	100%	100%
CPP-708 (stack)	100%	100%		100%	100%	100%
MFC-764 (stack)	100%	100%		100%	100%	100%
MFC-774	100%	100%		100%	100%	100%
NRF	100%	100%		100%	100%	100%
RWMC	100%	100%	100%	100%	100%	100%
TAN-679	100%	100%		100%	100%	100%
TRA-770 (stack)	97.5%	100%	100%	99.3%	98.3%	100%

Intensity						
Source	^{241}Am	^{137}Cs	^{3}H	^{238}Pu	^{239}Pu	^{90}Sr
ATR	44.8%	56.0%		46.1%	45.3%	58.3%
CFA-625	38.0%	49.5%		40.0%	38.8%	51.4%
CITRC	28.0%	49.6%		31.0%	29.2%	52.1%
CPP-1774	44.6%	55.5%	85.5%	46.0%	45.2%	57.6%
CPP-708 (stack)	11.3%	31.7%		13.4%	12.1%	35.4%
MFC-764 (stack)	5.05%	33.4%		6.5%	5.56%	40.9%
MFC-774	3.75%	10.5%		4.2%	3.92%	12.2%
NRF	49.1%	60.5%		50.8%	49.8%	62.7%
RWMC	32.1%	45.0%	69.1%	34.6%	33.3%	46.6%
TAN-679	8.22%	41.1%		10.5%	9.1%	46.7%
TRA-770 (stack)	6.19%	25.0%	79.2%	7.3%	6.7%	29.2%

Table 8. Frequency of detection for onsite samplers for ^{241}Am releases from six INL Site sources.

	Source					
Sampler	MFC-774	MFC-764	TRA-770	CPP-1774	RWMC	TAN-679
BEA-TRA	0.00%	1.00%	76.3%	97.1%	79.0%	1.70%
BEA-CPP	0.00%	0.00%	1.60%	99.8%	86.5%	6.40%
BEA-RWMC	0.00%	0.00%	0.00%	87.1%	100%	0.00%
BEA-VAN	0.00%	0.00%	3.80%	96.5%	99.2%	0.20%
BEA-SMC	0.00%	3.80%	0.00%	1.50%	0.00%	100%
BEA-GATE	0.00%	4.90%	0.00%	28.0%	0.00%	98.1%
BEA-ARA	7.60%	3.30%	0.00%	69.5%	20.7%	2.50%
BEA-REST	0.00%	1.20%	38.8%	88.9%	99.7%	0.00%
BEA-NRF	0.00%	0.00%	5.80%	95.3%	12.7%	14.1%
BEA-RTC	0.00%	1.10%	83.2%	98.6%	70.8%	2.70%
BEA-EBR	0.00%	0.00%	0.60%	94.6%	99.6%	0.20%
BEA-MFC	100%	99.4%	0.00%	11.9%	0.00%	3.90%
BEA-PBF	0.00%	0.20%	0.00%	94.4%	46.7%	7.00%
BEA-INTEC	0.00%	0.00%	0.10%	100%	80.8%	7.00%
BEA-CFA	0.00%	0.00%	0.30%	99.0%	89.1%	0.60%
BEA-EFS	0.00%	0.00%	3.40%	100%	50.3%	15.1%
ESER-VAN	0.00%	0.00%	3.80%	96.5%	99.2%	0.20%
ESER-FAA	17.9%	0.80%	0.00%	2.20%	0.00%	0.00%
ESER-MAI	0.00%	1.60%	0.00%	96.2%	58.3%	0.80%
ESER-EFS	0.00%	0.00%	3.00%	100%	50.2%	15.1%
ESER-ATO	9.50%	15.9%	0.00%	48.6%	13.4%	0.00%

Figure1

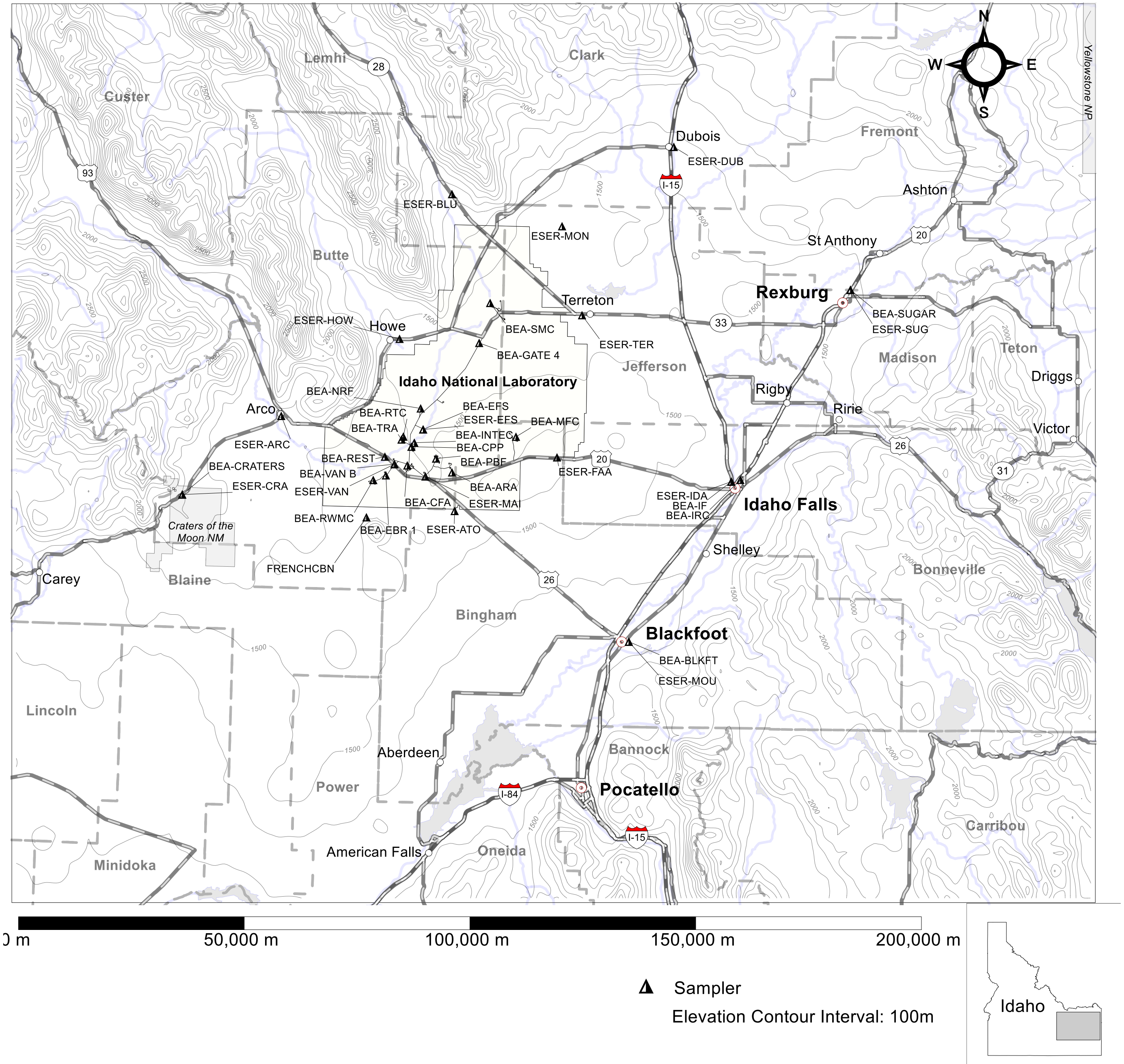

Fig. 1

Figure2

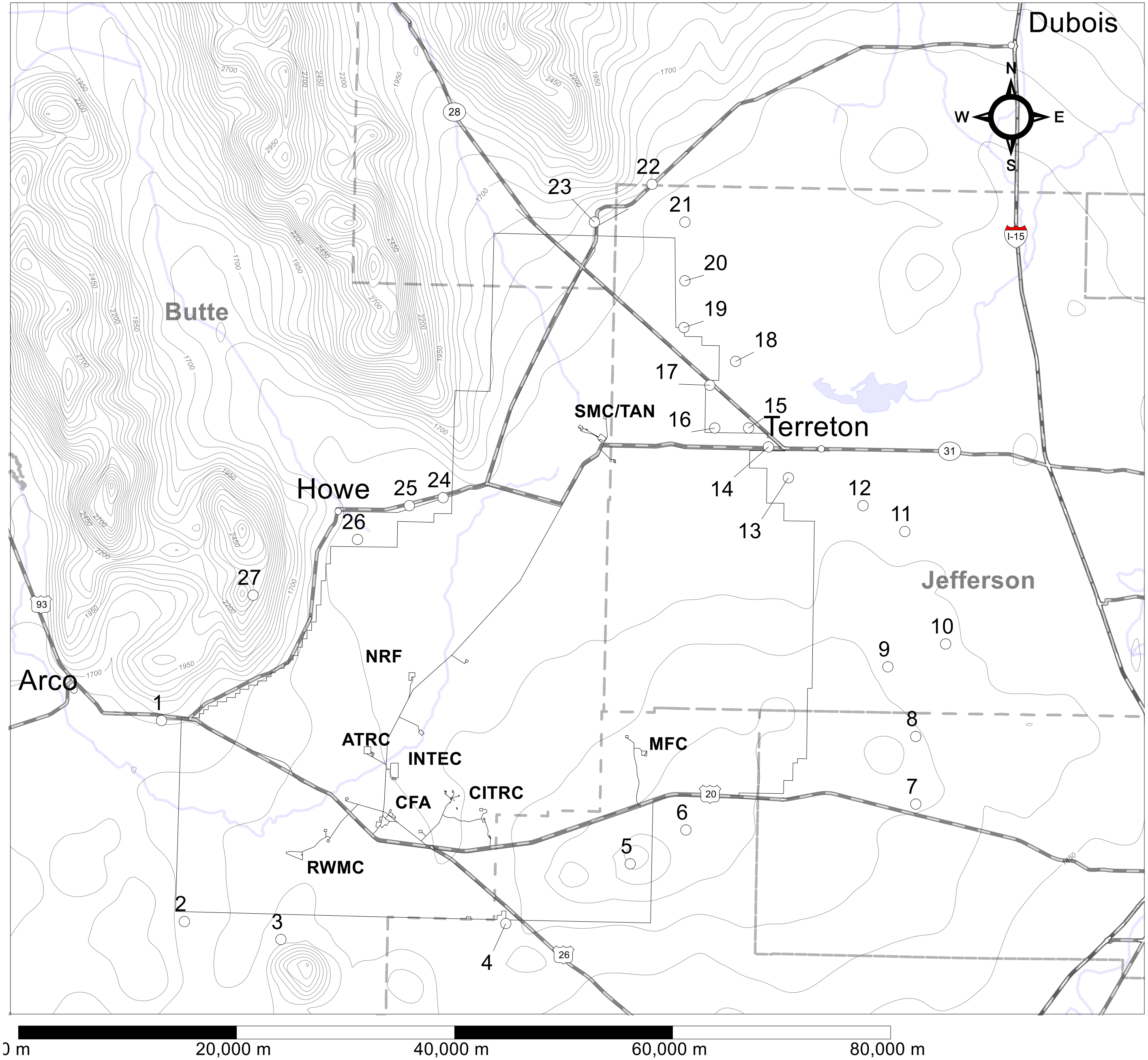

Fig. 2

Figure3

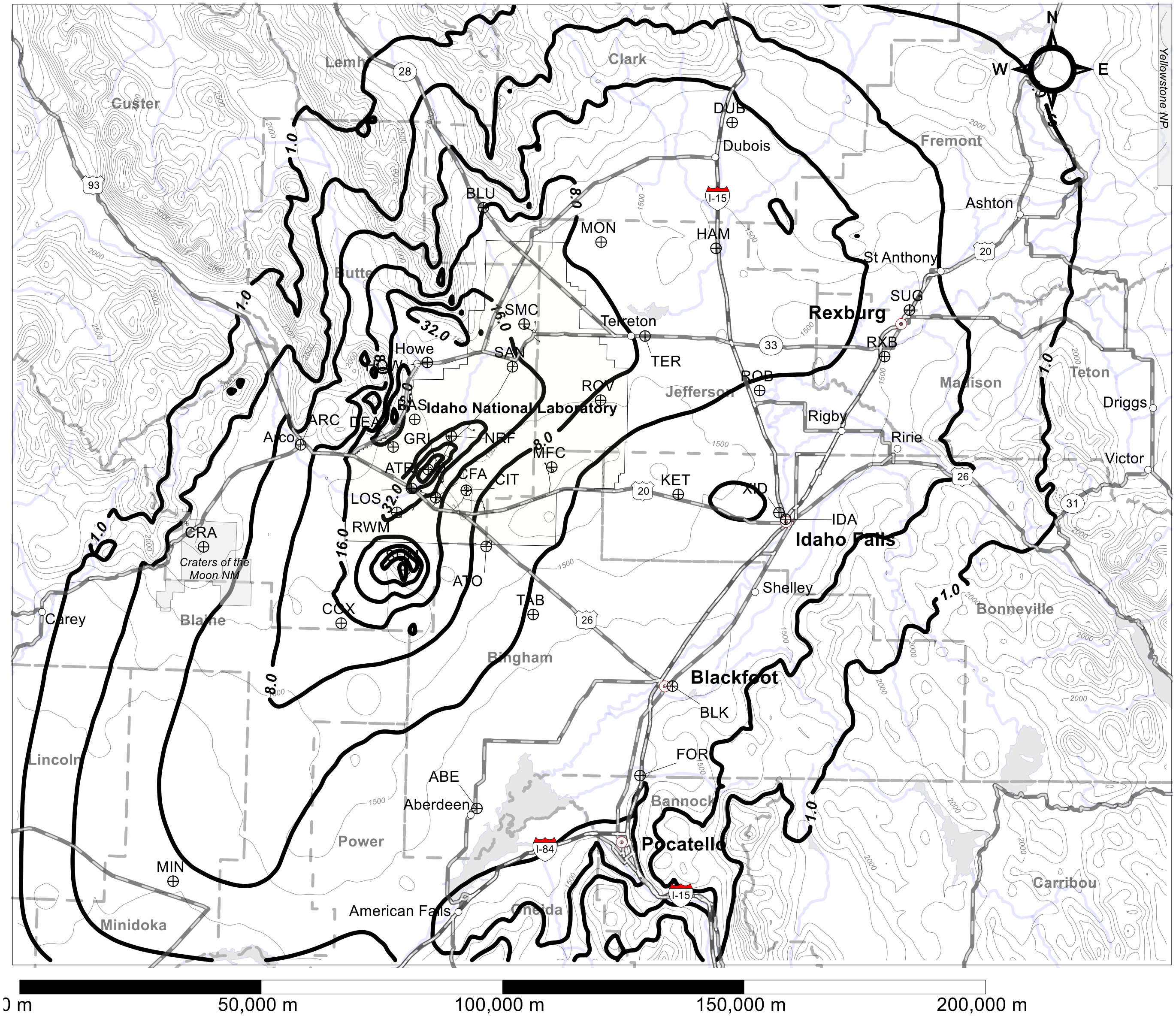

Fig. 3

Figure4

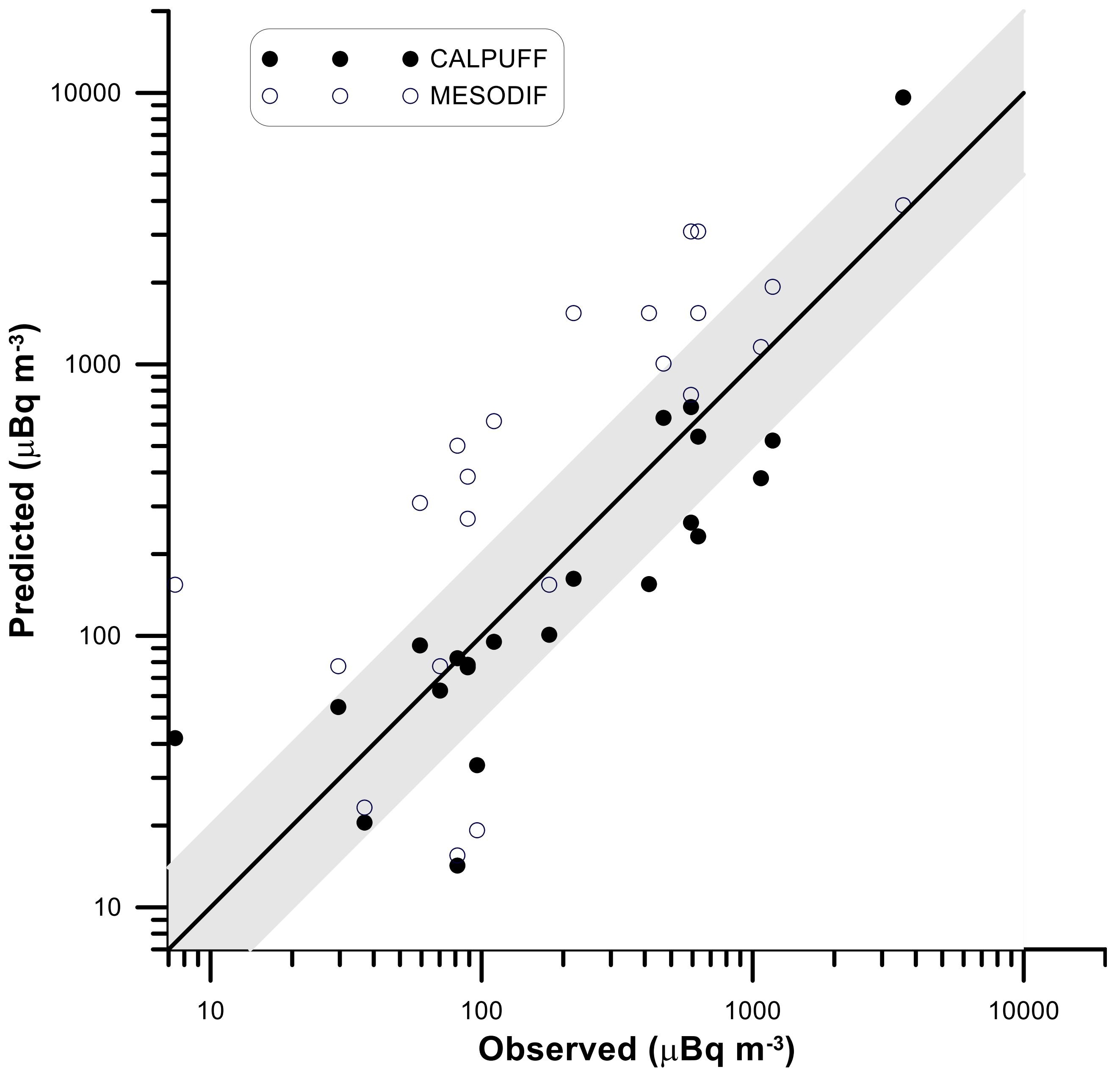

Fig. 4

Figure5

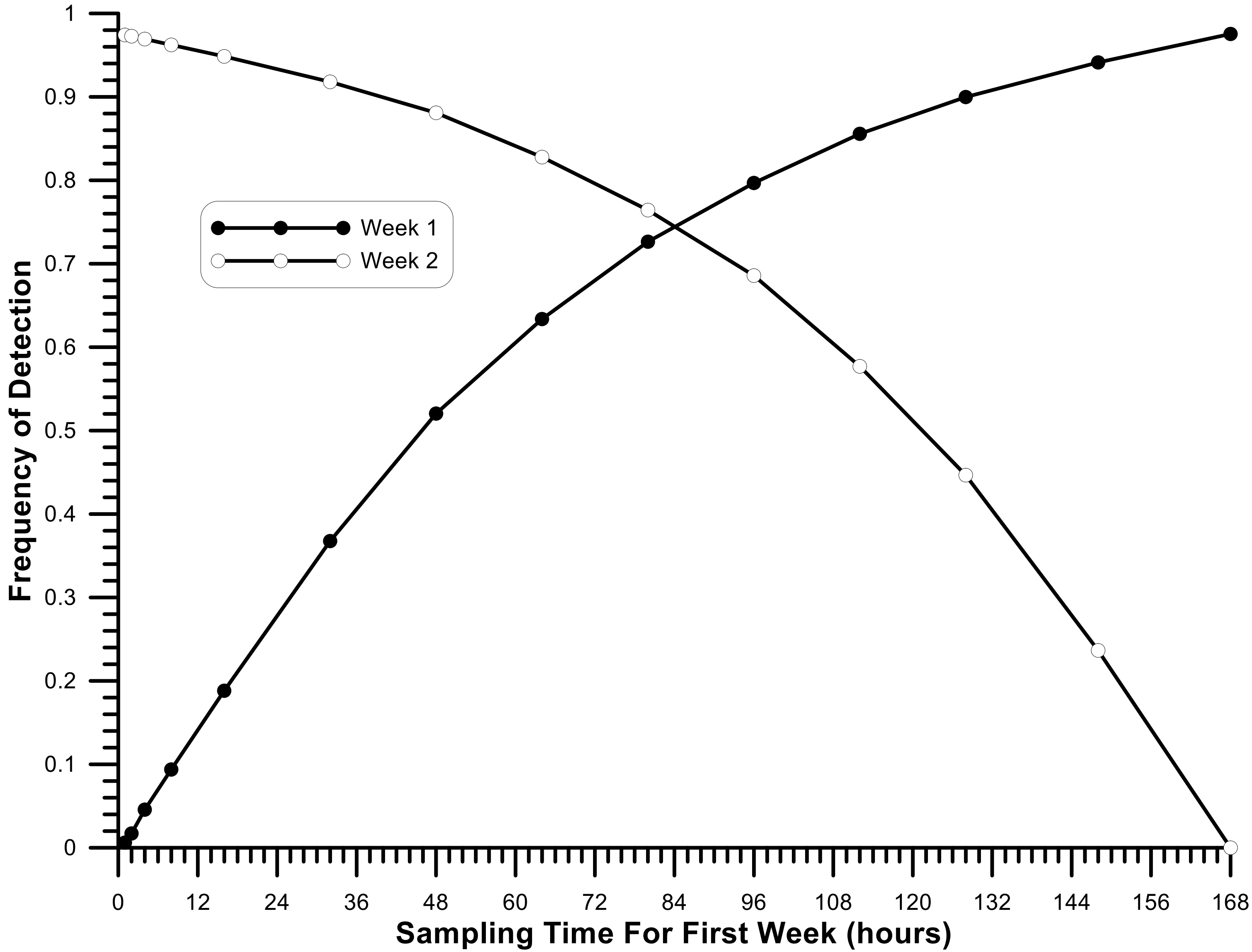

Fig. 5

Figure6

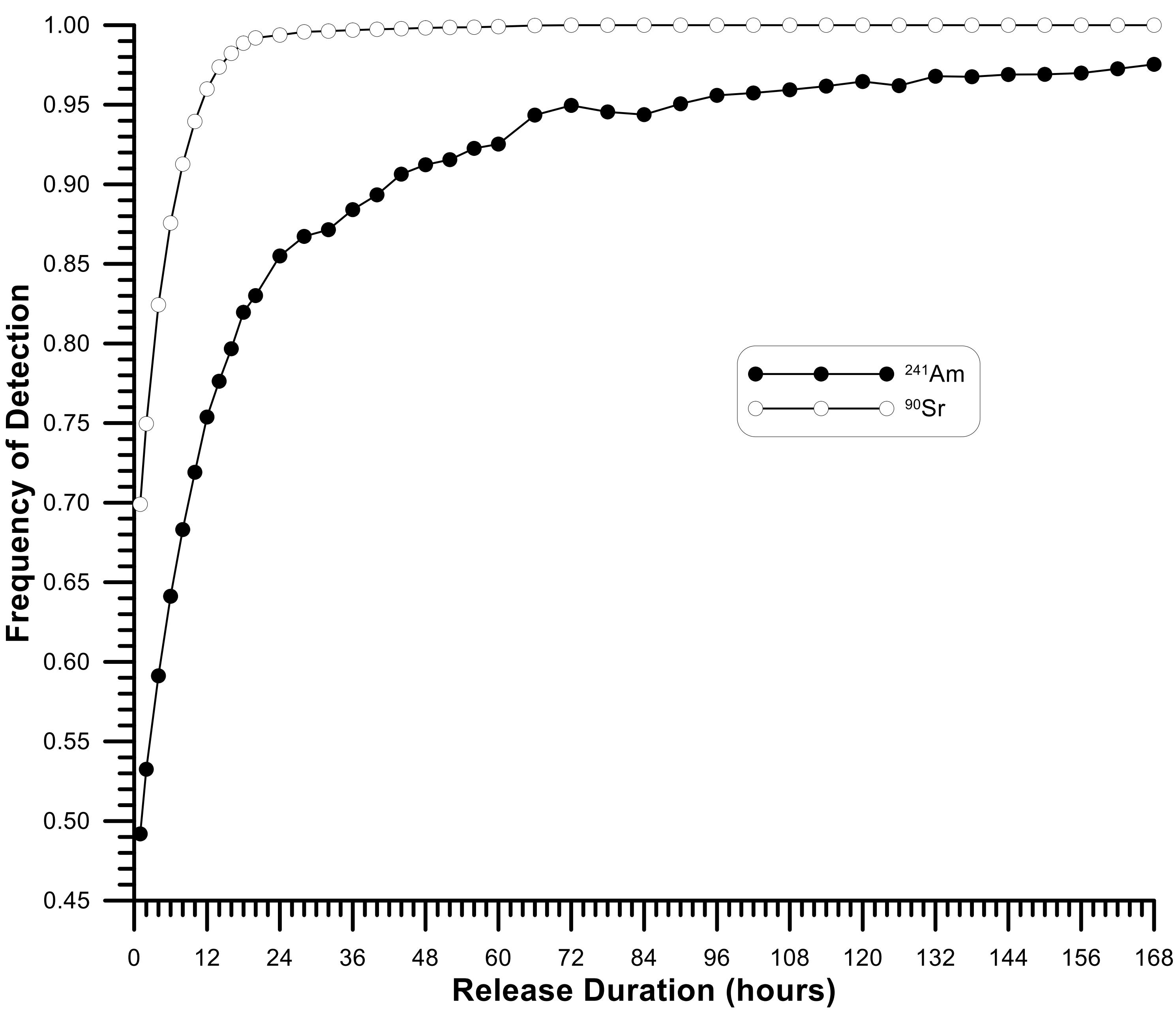

Fig. 6